Journal of University of Science and Technology Beijing
Vol.8(2001), No.1, p.6

Fluid Inclusions and Daughter Minerals of Taibai Gold Deposit, ShaanXi Province, China

Yuling Xie, Jiuhua Xu, Dayi Qian, Jianping Li

Resources Engeneering School, University of Science and Technology Beijing, Beijing 100083, China
(Received 2000-04-11)

Abstract: A discovery of daughter minerals in fluid inclusions of Taibai gold deposit, Shaanxi province has been focused on, which is a unique breccia-cemented gold-bearing system. The breccia zone strikes NWW-SEE, occurring in Devonian strata of Southern Qinling Mountains. The cement is mainly composed of ankerite, pyrite, calcite and quartz, which may be divided into four main tectonic-mineralizing stages. Gold mainly occurs in pyrite and ankerite of stage II and IV. It is found that three types of fluid inclusions can be distinguished: (1) aqueous inclusions (type B); (2) CO_2-rich inclusions (type C); (3) daughter minerals-containing inclusions (type A). LRM (Laser Raman Micro-probe) analyses shows that the content of CO_2 occupies 54.4%–70.7% (mole fraction, so as the follows) in vapor phases of different type fluid inclusions. CH_4 (5.2%–7.3%) and H_2S (6.0%–12.7%) exist in both vapor and liquid phases. Many daughter minerals in fluid inclusions of ankerite and quartz have been found. Several kinds of daughter minerals, including ankerite, pyrite, arsenopyrite and halite, were determined by using SEM (scanning electron microscope) / EDS (energy dispersive spectrometer) technique. EPMA (electron probe micro-analysis) technique was also applied to study the daughter minerals exposed to the surface of polished thin sections.

Key words: daughter minerals; fluid inclusions; gold deposit; breccia

Much progress in the study of daughter minerals in fluid inclusions has been made with the developing of SEM (scanning electron microscope) / EDS (energy dispersive spectrometer) and EPMA (electron probe micro-analysis) in recent years. The metallic daughter minerals reported frequently were chalcopyrite in higher saline aqueous inclusions of porphyry copper deposits [1–7]. Next were sphalerite, chalcopyrite and pyrite [8, 9] in fluid inclusions of volcanic massive sulfide deposits. However, the daughter minerals in fluid inclusions of hydrothermal gold deposits have rarely been reported. This paper focuses on the fluid inclusion study and discovery of pyrite and ankerite daughter minerals of Taibai gold deposit, which is a unique breccia-cemented gold-bearing system.

1 Geological Setting and Fluid Inclusions Characteristics

Taibai gold deposit, located in Shaanxi province, occurs in Devonian gold-bearing breccia zone of Southern Qinling Mountains. The breccia zone strikes NWW-SEE within middle Devonian of ankeritic, siltic, sericite slate and albitic slate. The breccias are composed of these metamorphic wallrocks. The size of breccia is variable, from several centimeters to several meters. The cement is mainly composed of ankerite, pyrite, calcite and quartz, which may be divided into six tectonic-mineralizing stages. Gold mainly occurs in pyrite and ankerite of stage II and IV.

There are a great number of fluid inclusions in ankerite and quartz of main mineralizing stages (shown as **figure 1**). They are irregular or negative crystal shaped and less than 2 μm to 15 μm in size. Three types of fluid inclusions can be distinguished: (1) aqueous inclusions (type B, figure 1 (B)) are composed of one liquid phase and one vapor phase; (2) CO_2-rich inclusions (type C, figure 1 (C)) are composed of an aqueous phase, CO_2 liquid phase and CO_2 vapor phase. Some inclusions have no aqueous phase, forming pure CO_2 inclusions. CO_2 liquid may homogenize into one phase at high room temperature; (3) fluid inclusions containing daughter minerals can be usually found in ankerite and quartz (figure 1 (A)). The daughter minerals are mainly pyrite, halite and ankerite, detected by Electron Microprobe analysis and SEM/EDS (as mentioned later).

2 LRM (laser Raman micro-probe) Analyses of Fluid Inclusions

LRM analyses have been made for type A, B and C inclusions (**table 1**). The main results are as follows.

(1) CO_2 occupies larger portions in vapor phases of different type fluid inclusions, between 54.4%–70.7% (mole fraction, so as the follows), but they are lower

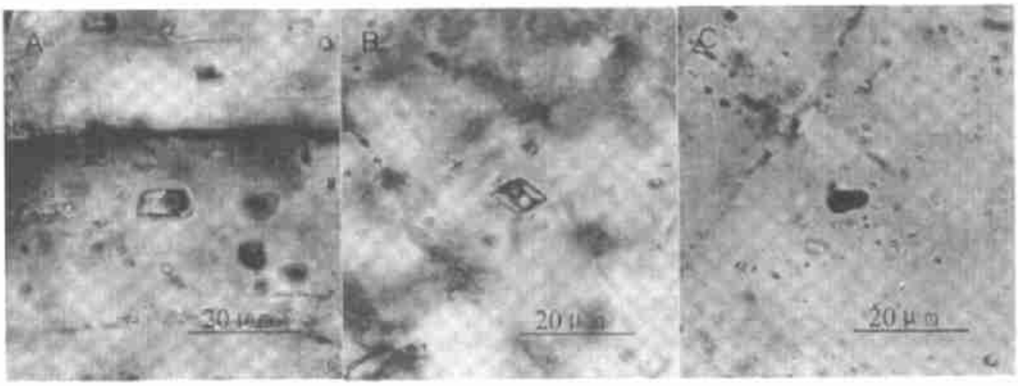

Figure 1 Photographs of fluid inclusions containing daughter minerals from Taibai gold deposit, (A) fluid inclusions containing daughter minerals of carbonate; (B) fluid inclusions containing daughter minerals of halite, (C) fluid inclusions containing daughter minerals of sulfide.

Table 1 LRM analyses of fluid inclusions of Taibai gold deposit (mole fraction in %)

Sample	Host mineral	CO_2	N_2	H_2S	CH_4	H_2O	SO_2	CO	CO_2 / CH_4	CO_2 / H_2O	Type of FI.
T577	Ank	44.1	7.6	L	5.3	36.5	L	L	8.32	1.21	A, Vapor
		21.7	—	L	6.1	63.8	8.4	—	3.56	0.34	Liquid
T417-1	Ank	55.0	L	6.0	5.2	L	10.0	23.8	10.57	L	B, Vapor
		59.5	—	7.4	8.8	24.3	L	—	6.76	2.45	Liquid
T417-2	Ank	70.0	L	L	7.0	22.3	L	L	10.10	3.17	C
T511-1	Q	48.3	15.4	12.7	7.3	16.3	L	L	6.62	2.96	B, Vapor
		65.0	—	10.3	L	24.6	L	—	L	2.64	Liquid
T511-2	Ank	54.4	L	11.1	L	9.9	L	24.6	L	5.50	C

Note: (1) The data were analyzed by Zhihai Wang and Yueqin Li of Institute of Geology and Mineral Resources, Xi'an; (2) Instrument: RAMANOR U1000; (3) Experiment conditions: Ar^+ Laser, Wavelength 514.5 nm, Laser power 600 mW, Narrow seam 450 μm; (4) Ank: ankerite; Q: quartz; (5) "L": less than measurable limit; "—": unmeasured.

than those from Xiaoqinling greenstone-type gold deposits (57.4%–85.4%). Vapor phases contain H_2O(g), between 9.9%–36.5%. Type A inclusions have higher H_2O(g) than type B and type C inclusions; the type C inclusions have the lowest H_2O(g). This is in content with the CO_2 solubility in saline solution. The content of H_2O(g) in vapor phase of fluid inclusions in TaiBai gold deposit was detected to be up to 36.5, while no water was found in vapor phases of inclusions from Xiaoqinling [10]. CO_2/H_2O (g) of vapor phase of fluid inclusion is 1.21%–5.50%, and increases from type A, B to C inclusions.

(2) The H_2O(l) content of liquid phase in type A inclusions are higher than that of the type B, while the CO_2 content is reverse. Like those in vapor phases, CO_2/ H_2O of liquid phases of fluid inclusions increases from A, B to C, reflecting that the ore-forming fluids had evolved from higher saline to CO_2-rich.

(3) CH_4 (5.2–7.3) and H_2S (6.0–12.7) exist in both vapor and liquid phases; CO and SO_2 are also detected in some samples.

3 SEM/EDS and EPMA Study of Daughter Minerals

There are many daughter minerals in fluid inclusions of ankerite (Fe/Mg<1, mass ratio) and quartz, including transparent and nontransparent ones. The transparent daughter minerals have an automorphous crystal shape. Some cubic minerals are halite because of the dissolving among 260–265 ℃. However, some daughter minerals having rhombic shape are not melted when heated to 500–570 ℃. Several kinds of daughter minerals were found by using SEM/EDS technique (**figure 2**). The rhombic daughter minerals, having higher Ca, Mg and Fe peak values of energy spectrum, are ankerite, with 0.833–0.729 of (Mg+Fe)/Ca (mass ratio) and 1.06–1.27 of Fe/Mg (mass ratio) (**table 2**). Those with complex types were detected to be ankerite and halite. Some nontransparent daughter minerals are pyrite and arsenopyrite.

EPMA technique was also applied to study the daughter minerals exposed to the surface of polished thin sections. The result shows that the daughter minerals with bright yellow color under reflecting microscope are pyrite (**table 3**). No pyrrhotite was found, so

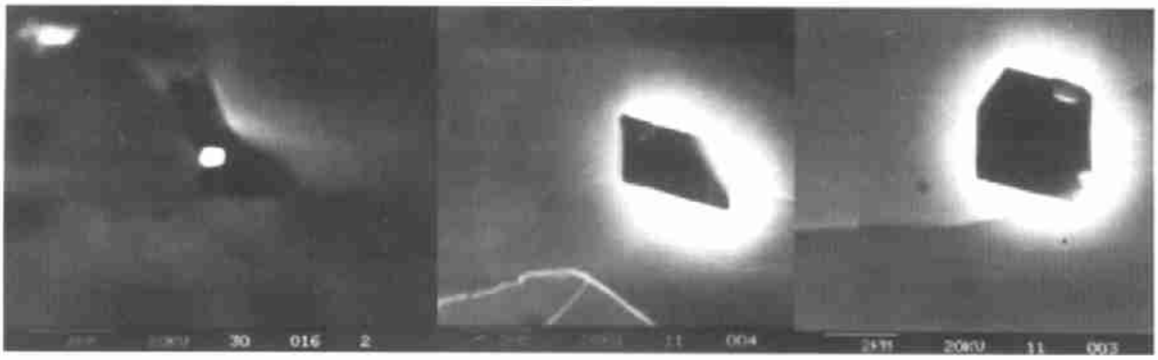

(A) (B) (C)

Figure 2 Phtographs of daughter minerals in fluid inclusions of ferro-dolomite from Taibai gold deposit, (A) Pyrite daughter minerals in ferro-dolomite; (B) and (C) Ankerite daughter minerals in ferro-dolomite.

Table 2 SEM/EDS analyses of daughter minerals in fluid inclusions from Taibai gold deposit

Sample	T440-2		T210-1		T210-2		T210-3		T552-2	
	w / %	*x* / %	*w* / %	*x* / %	*w* / %	*x* / %	*w* / %	*x*	*w* / %	*x* / %
Fe	30.851	30.259	46.14	32.96	—	—	23.129	15.390	23.59	16.06
S	19.872	33.953	53.86	67.04	—	—	0.158	0.183	—	—
Na	—	—	—	—	35.05	45.00	0.00	0.000	—	—
Cl	—	—	—	—	64.95	55.00	0.903	0.947	—	—
Si	—	—	—	—	—	—	0.352	0.466	—	—
Ca	—	—	—	—	—	—	53.785	49.871	57.84	54.89
Mg	—	—	—	—	—	—	21.681	33.143	18.57	29.05
Zn	0.550	0.46	—	—	—	—	—	—	—	—
As	47.882	35.009	—	—	—	—	—	—	—	—
Te	0.557	0.239	—	—	—	—	—	—	—	—
Pb	0.296	0.078	—	—	—	—	—	—	—	—
Total	100.008	100.00	100.00	100.00	100.00	100.00	100.008	100.00	100.00	100.00
HM	Quartz		Ankerite (Fe/Mg<1)		Ankerite (Fe/Mg<1)		Ankerite (Fe/Mg<1)		Ankerite (Fe/Mg<1)	
DM	Arsenopyrite		Pyrite		Halite		Ankerite (Fe/Mg>1)		Ankerite (Fe/Mg>1)	

Note: (1) SEM/EDS instrument: S-250MK3, AN10000; distinguishable 5nm; (2) "—": not detected; (3) HM: host mineral, DM: daughter mineral; (4) *w*: mass fraction, *x*: atom fraction.

Table 3 EPMA analyses of daughter minerals in fluid inclusions of ankerite from Taibai gold deposit

Sample		Fe	S	Co	Ni	Zn	As	Te	Au	Ag	Pt	Total	DM
T590*	*ω* / %	45.73	53.40	0.05	0.00	0.16	0.14	0.19	0.13	0.06	0.13	100.00	Pyrite
	x / %	32.84	66.81	0.04	0.00	0.10	0.08	0.06	0.03	0.02	0.03	100.00	
F15*	*ω* / %	45.88	52.35	0.20	0.62	0.27	0.46	0.12	0.00	0.10	0.00	100.00	Pyrite
	x / %	33.11	65.83	0.14	0.43	0.17	0.25	0.04	0.00	0.04	0.00	100.00	

Note: (1) The data were analyzed by Shuyan Li of China University of Geosciences; (2) Instrument: JCXA-733 Electron Microprobe and Link 860-2 Energy Spectrometer; 15 kV, wave length 2×10^{-7} nm; Diameter of excited beam 0.5 μm; Mean error: <1%; (3) DM: daughter mineral; (4)*: calculated by excluding impurities from elements of host mineral; (6) *w*: mass fraction, *x*: atom fraction.

it is indicated that ore-forming fluid was formed under a relative oxidation condition. This also suggested by sulfur components obtained from LRM analyses, mineral assemblage of gold mineralization and tension characteristics of breccia zone.

4 Stable Isotope Data and Source of Ore-forming Fluids

In recent years, much data on stable isotopes has been accumulated on ankerite, pyrite and quartz of Taibai gold deposit. The range of $\delta^{18}O$ of quartz and albite is from 16.56‰ to 19.90‰, and that of ankerite is from 15.06‰ to 18.66‰. While that of calcite is from 7.5‰ to 14.86‰ [11]. Our data shows that the $\delta^{18}O$ values of ankerite vary slightly, that is, from 17.55‰ to 19.64‰ (9 samples). The calculated $\delta^{18}O$ of fluid inclusions may change from 8.32‰ to 15.20‰, when using the quartz-H_2O and dolomite -H_2O fractionation equations.

The values of δD of inclusion fluids in quartz are within the range of −65.4‰ to −131.9‰. The other similar range (−62.2‰ to −76.7‰) has been reported by Shi Z. et al. [11]. The ankerite $\delta^{13}C_{PDB}$ values of this study are from −5.20‰ to −6.74‰, which is within the range of −4.47‰ to −7.89‰ reported by Shi Z. et al. [11]. It may be concluded that the water in the hydrothermal fluids during main gold mineralizing stages could have been a mantle source, according to the $\delta^{13}C$ values and the field of magnetic water suggested by Taylor [12]. However, local meteoric water might have been important in late mineralization, because of the lower δD.

5 Conclusions

(1) Three types (A, B, C) of fluid inclusions can be distinguished in ankerite and quartz from main mineralizing stages. Fluid boiling existed during the second stage.

(2) Many daughter minerals in fluid inclusions of ankerite and quartz have been found. Several kinds of daughter minerals, including ankerite, pyrite, arsenopyrite and halite, were determined by using SEM/EDS and EPMA technique.

(3) The characteristics of ore-forming fluids which is different from either lode gold deposits in Archean greenstone terrains or the Carling-type gold deposits show that TaiBai gold deposit is formed in complex physical and chemical condition.

Acknowledgment

The research is aided by the financial support from National Natural Science Foundation of China (49972031), University of Science and Technology Beijing and TaiBai Gold Mine. The authors thank Profs. He Zhili, Shuyan Li and Qianmao Li for their great helps.

References

[1] J. A. Mavrogenes, R. J. Bodnar: *Geochim. Cosmochim. Acta.*, 58 (1994), p. 141.
[2] S. J. Meldrum, R. S. Aquino, R. I. Gonzales, et al.: *J. Geochem. Explor.*, 50 (1994), p. 203.
[3] B. Stefanini, A. E. Willams Jones: *Economic Geol.*, 91 (1996), p. 774.
[4] B. Iriato, G. H. Clark: [In:] *Abstract of PACRIM'95*, Indonesia, 1995, p. 299.
[5] J. R. Kyle, R. J. Bodnar: *Geol. Soc. Am.*, 27 (1995), PA-65.
[6] P. Chen, X. Chen, P. Ni, et al.: *Chinese Science Bulletin* (in Chinese), 41 (1996), p. 632.
[7] I. Pintea: *Abstract of ECROFI VIII*, 18 (1995), p. 184.
[8] Khin Zaw, J. B. Gemmell, R. R. Large, et al.: *Ore Geol. Review*, 10 (1996), p. 251.
[9] W. Liu, R. Zhen, Y. Li, et al.: *Journal of Chengdu University of Technology* (in Chinese), 24 (1997), p. 65.
[10] J. Xu: China. Resour. *Geol., Special Issue* (1993), No.16, p. 328.
[11] Z. Shi, J. Liu, D. Ju, et al.: *Contributions to the Gold Deposit Geology of Eastern China* (4. Eastern Qinling Area) (in Chinese), Geological Publishing House, 1993, p. 35.
[12] H. P. Taylor, Jr.: [In:] *Geocemistry of Hydrothermal Ore Deposits*, H. L. Barnes [eds.:], Wiley Interscience, New York, 1979, p. 236.